



# Softening Resistance, Dimensional Stability and Corrosion Behaviour of Alumina and Rice Husk Ash Reinforced Aluminium Matrix Composites Subjected to Thermal Cycling

K.K. Alaneme<sup>a</sup>, Y.O. Anabaranze<sup>a</sup>, S.R. Oke<sup>a</sup>

<sup>a</sup>Department of Metallurgical and Materials Engineering, Federal University of Technology, Akure, PMB 704, Nigeria.

## Keywords:

Aluminium hybrid composites  
Corrosion resistance  
Dimensional stability  
Rice husk ash  
Softening resistance  
Alumina

## ABSTRACT

The softening resistance, dimensional stability and corrosion behaviour of stir cast alumina and rice husk ash reinforced aluminium matrix composites subjected to thermal cycling has been investigated. Aluminium hybrid composites having 10 wt% reinforcement consisting of alumina ( $Al_2O_3$ ) and rice husk ash (RHA) in weight ratios of 1:0, 3:1, 1:1, 1:3, and 0:1 respectively were produced. The composites were subjected to varying thermal cycles of 3, 6, 9 and 12 from room temperature to 200 °C repeatedly. Hardness, linear change in dimensions, microstructural examination and corrosion test were used to characterize the composites produced. From the results, no obvious change in the microstructure could be discerned with thermal cycling. There were only marginal changes in hardness with increase in thermal cycling also less than 2 % change in linear dimensions was observed with thermal cycling. The composites were also observed to be very resistant to corrosion in 3.5 % NaCl solution with no appreciable change in corrosion resistance noted with increase in thermal cycling. However, in 0.3M  $H_2SO_4$  solution, the corrosion resistance increased with increase in RHA content and samples subjected to 9 and 12 thermal cycles exhibited a relatively higher susceptibility to corrosion.

## Corresponding author:

Kenneth K. Alaneme  
Department of Metallurgical and  
Materials Engineering,  
Federal University of Technology,  
Akure, PMB 704, Nigeria.  
E-mail: kalanemek@yahoo.co.uk

© 2015 Published by Faculty of Engineering

## 1. INTRODUCTION

The design of Aluminium matrix composites (AMCs) has continued to attract the interest of researchers as a result of its good combination of properties. Properties such as high specific strength, high specific stiffness, low thermal coefficient of expansion, improved tribological properties and low cost of processing; has been

responsible for its rapid development over the years [1-3]. These properties coupled with excellent corrosion resistance and thermal stability makes them an excellent choice for design of components for automobile, aerospace, electronic, and thermal management applications [4-5]. Thus on account of the economic, environmental and technical performance benefits of AMCs, they have been

considered first choice materials ahead of other competing materials for the design of a wide range of components and parts [6]. Components such as ventral fins, rotating blade sleeves, gear parts, crankshafts, integrated heat sinks, microwave housing, and fuselage frames among others have been successfully designed with the use of AMCs [7].

In some of the applications where AMCs are utilized, they are exposed to fluctuating thermal loads in service and are still expected to maintain operational functionality [8]. Under such conditions, thermal and structural stability are critical to component performance and longevity. In order to avert under performance and premature failure of AMCs in such environments their behaviour under such conditions needs thorough evaluation at the material design stage.

Several studies have been carried out to study the material behaviour of aluminium matrix composites exposed to varied thermal operating conditions [9-11]. The respective coefficient of thermal expansion of the reinforcement(s) and the matrix, the volume fraction of both phases, and other material characteristics of the composite constituents; have been identified to influence the thermal, structural and mechanical stability of the composites in service [12]. Generally, for composites reinforced solely with SiC, alumina and boron, the thermal and structural stability levels have been assessed as very good prompting their use in thermal management applications [13].

Recently ashes derived from controlled burning of agro wastes such as coconut shell, bamboo leaf, bagasse among others have been used along with traditional ceramic reinforcing materials (such as SiC and alumina) to develop Aluminium based composites [14]. The suitability of rice husk ash as a complement to alumina and SiC as hybrid reinforcement in Aluminium matrix composites has also been reported by several authors [15-16]. The material behaviour of these hybrid reinforced AMCs has been very promising [17], but their suitability for thermal management applications has received limited attention from researchers. For such applications the components undergo repeated heating and cooling cycles which can alter component performance in service. In the

present research the influence of thermal cycling on the softening resistance, dimensional stability and corrosion behaviour of alumina-rice husk ash hybrid reinforced aluminium matrix composites is reported.

## 2. MATERIALS AND METHOD

### 2.1 Materials

Al-Mg-Si alloy (AA 6063 grade) was selected as the matrix for the production of the composites. Chemically pure Alumina ( $Al_2O_3$ ) particles and rice husk ash (RHA) both having average particle sizes of 30 and 50  $\mu m$  respectively were selected as reinforcements for the Aluminium based composites to be produced. The preparation of the RHA from rice husk and subsequent conditioning treatment has been reported in details by Alaneme and Adewale [17]. The chemical compositions of the Al-Mg-Si based alloy and RHA used in the composite production are presented in Tables 1 and 2 respectively.

**Table 1.** Chemical Composition of the Al-Mg-Si alloy.

Element	wt (%)
Al	98.84
Si	0.3774
Fe	0.1682
Cu	<0.002
Mn	0.0127
Mg	0.4648
Zn	<0.002
Cr	<0.002
Ni	0.0000
Ti	0.0163
V	<0.008

**Table 2.** Chemical Composition of the Rice Husk Ash.

Compound/Element	wt (%)
SiO <sub>2</sub>	91.59
C	4.8
CaO	1.58
MgO	0.53
K <sub>2</sub> O	0.39
Fe <sub>2</sub> O <sub>3</sub>	0.21
Na	trace
TiO <sub>2</sub>	0.20

### 2.2 Production of the Al Based Composites

Double stir casting process in accordance with Alaneme and Adewuyi [18] was adopted for the production of the composites. Preliminarily charge calculations were used to determine the quantities of Aluminium, rice

husk ash (RHA) and alumina (Al<sub>2</sub>O<sub>3</sub>) needed to achieve the desired composite compositions. In this regards, 10 wt% of different reinforcement mix consisting of RHA and Al<sub>2</sub>O<sub>3</sub> in weight ratios 0:1, 1:3, 1:1, 3:1, and 1:0 were prepared. The rice husk ash and alumina particles were initially preheated separately at a temperature of 250 °C to eliminate dampness and improve wettability with the molten Al-Mg-Si alloy. The Al-Mg-Si alloy was charged into a temperature controlled crucible furnace, and heated to a temperature of 750 °C ± 30 °C (above the liquidus temperature of the alloy) to ensure homogeneous and complete melting of the alloy. The liquid Al-Mg-Si alloy was then cooled in the furnace to a semi solid state holding at a temperature of about 600 °C. The preheated alumina and RHA was added at this temperature and the mix stirred manually for 5 minutes. The semi-solid composite formed was then superheated to 780 °C ± 30 °C and a second stirring performed using a mechanical stirrer. The stirring operation was performed at a speed of 400 rpm for 10minutes to help improve the distribution of the alumina and RHA particles in the molten Al-Mg-Si alloy based composite. The molten composite was then cast into prepared sand moulds fitted with metallic chills.

### 2.3 Thermal Cycling

The composites produced were subjected to 3, 6, 9 and 12 repeat heating to 200 °C for 45 minutes and air cooling cycles. The thermal cycling treatment was performed using a digital temperature controlled laboratory Oven having tolerance of ± 2° C. Samples which were not subjected thermal cycling treatments were also prepared for control experimentation. The sample designations for the varied composite compositions produced and subjected to thermal cycling are presented in Table 3.

**Table 3.** Thermal Cycles performed at 200 °C for 45 minutes followed by air cooling.

Sample Designation	Composition Al <sub>2</sub> O <sub>3</sub> : RHA	No. of Thermal Cycles
A1	1:0	
A10		0
A13		3
A16		6
A19		9
A112		12
A2	3:1	

A20		0
A23		3
A26		6
A29		9
A12		12
A3	1:1	
A30		0
A33		3
A36		6
A39		9
A312		12
A4	1:3	
A40		0
A43		3
A46		6
A49		9
A412		12
A5	0:1	
A50		0
A53		3
A56		6
A59		9
A512		12

### 2.4 Softening Resistance and Thermal Stability Evaluation

The softening resistance and thermal stability of the composites to alternating heating and air cooling cycles was evaluated by hardness and dimensional stability measurements. The hardness of the composites was evaluated using an EmcoTEST DURASCAN Microhardness Tester equipped with ecos workflow ultra modern software. Sample surface preparation to obtain a flat and smooth surface finish was performed on representative samples cut out from each composite composition produced prior to hardness testing. A load of 100 g was applied on the specimens and the hardness profile was evaluated using a Vickers hardness scale and procedures recommended in ASTM E 92-82 standard [19]. Repeat hardness tests were performed on each sample and the average of values taken within the range of ± 2 % was recorded as the hardness of the specimen. The dimensional stability of the composites was evaluated by adaptation of test procedures specified in ASTM D1204 standard [20]. The linear dimensional changes of the samples after repeat thermal cycles were measured and the dimensional stability determined using the relation:

$$\% \text{ linear dimension change} = \{(\text{final length} - \text{original length}) \div \text{original length}\} \times 100 \quad (2.1)$$

## 2.5 Microstructural Examination

The microstructures of the composites were examined using a JSM Jeol ultra-high resolution field emission gun scanning electron microscope (FEG-SEM). The surfaces of the samples for microstructural examination were metallographically prepared by grinding and polishing until a mirror like finish was produced on the sample surfaces. The samples were etched in Keller's reagent (95 ml water, 2.5 ml HNO<sub>3</sub>, 1.5 ml HCl, 1.0 ml HF) before the microstructural investigation.

## 2.6 Corrosion Test

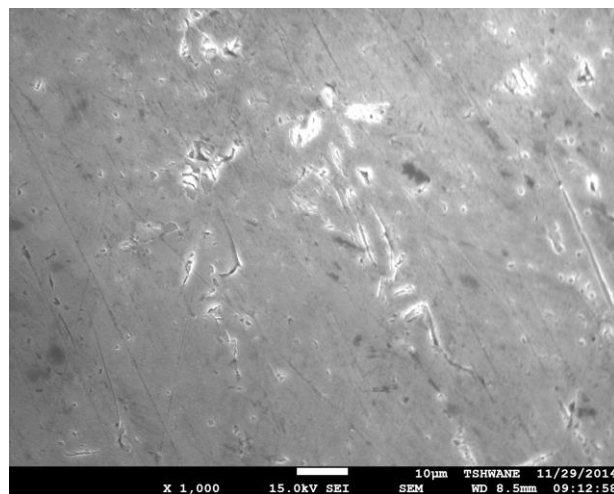
Weight loss method was used to assess corrosion behaviour of the composites produced. The corrosion test was performed by immersion of the specimens in stagnant 0.3 M H<sub>2</sub>SO<sub>4</sub> and 3.5 % NaCl solutions at room temperature. The sample preparation and testing procedures was performed in accordance with ASTM G31 [21] standard. In this regards, the test samples were mechanically polished, degreased with acetone, washed in distilled running water, and dried in air before the sample initial weighs are measured and then immersed in the corrosion media. The solution-to-specimen surface area ratio was about 150 ml cm<sup>-2</sup>, and the corrosion setups were opened to atmospheric air for the duration of the immersion test. The weight loss measurements were taken at intervals of three days of exposure in the media for a total of 45 days. The samples after withdrawal from the test solutions are rinsed with distilled water and the corrosion products removed from the samples by chemical cleaning in accordance with ASTM G31 standard recommended practice [21]. The mass losses (g/cm<sup>2</sup>) of the samples were determined by dividing the successive cumulative weight loss readings with the surface area of the samples.

## 3. RESULTS AND DISCUSSION

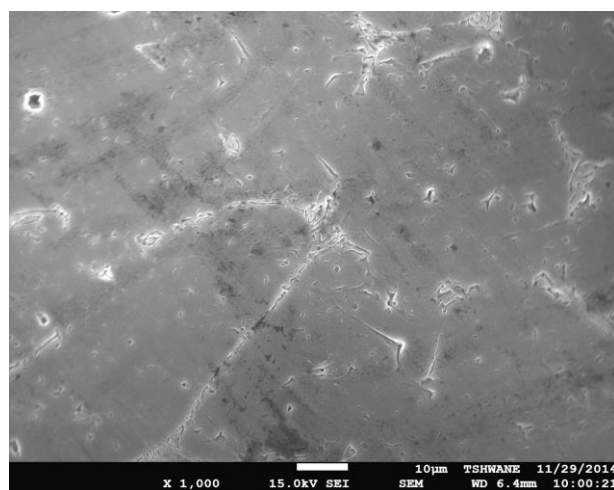
### 3.1 Microstructure

Figure 1 shows a representative set of microstructures of the composites produced before and after a number of repeated heating and cooling thermal cycles. It is observed from the micrographs that the reinforcing particles

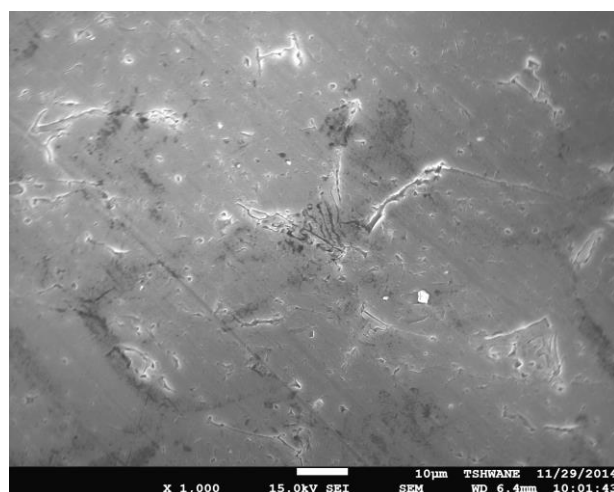
are visible and fairly distributed in the Al-Mg-Si matrix (continuous phase).



(a)



(b)



(c)

**Fig. 1.** Representative microstructures of the Al-Mg-Si based Composites containing 75 % alumina and 25 % RHA (A2) (a) no thermal cycling (A20), (b) after 6 thermal cycling (26), and (c) after 12 thermal cycling (A12).

However, any effect of the thermal cycling treatment on the microstructure of the composites was not clearly apparent. The Al-Mg-Si alloy matrix and the refractory reinforcing particles did not show any visible change of significance. This same trend was consistent for all composite series produced hence the use of representative samples to explain the observation noted.

### 3.2 Softening resistance and dimensional stability

Figure 2 shows the variation of hardness of the composites produced before and after thermal cycling. The hardness measure was the most convenient and reliable measure of the softening resistance of the composites. As expected, the hardness of the composites decreased with increase in the RHA content, which is clearly due to the high silica content in RHA (Table 2). Silica is noted to be a softer refractory ceramic compared to alumina [22]. It was however noted that for each composite series (A1, A2, A3, A4, and A5) the hardness only exhibited marginal changes in value with increase in thermal cycles. This is an indication that the composites have good resistance to softening and maintains to a reasonable extent its structural integrity when exposed to repeated heating and cooling cycles. This attests to the fact that the composites will be reliable and suitable for use in thermal management applications.

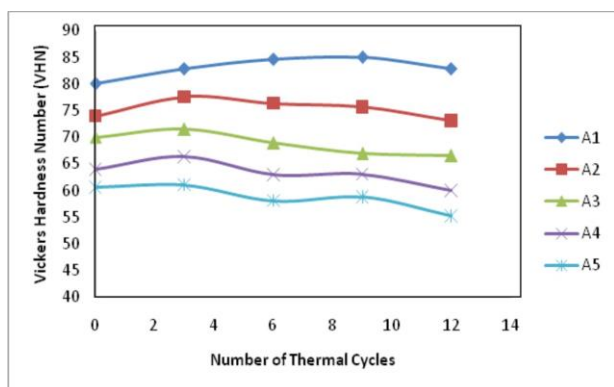


**Fig. 2.** Variation of hardness of the composites before and after thermal cycling.

It was also observed that the hybrid mix of RHA and alumina does not affect the dimensional stability capacity of the Al-Mg-Si alloy based composites. This fact is confirmed from observations of the linear dimensional changes of the composites after thermal cycling (Table 4). It is observed from the table that percent

change in linear dimensions of the samples after 6 and 12 cycles (which were the intermediate and maximum number of repeat heating and cooling cycles the samples were subjected to was less than 2 %. This indicates that the use of RHA as complementary reinforcement to alumina in the AMC development does not alter the thermal stability potentials of the composites hence they remain very suitable for the design of Aluminium based composites for thermal management applications.

**Table 4.** Dimensional Stability Results for the Composites produced after 6, 12 thermal cycles.

Sample Designation	Dimensional Stability (% change in linear dimension)
For 6 Thermal Cycles	
A16	0.49 ± 0.04
A26	1.15 ± 0.08
A36	1.68 ± 0.05
A46	1.29 ± 0.03
A56	1.17 ± 0.08
For 12 Thermal Cycles	
A112	1.39 ± 0.04
A212	1.54 ± 0.08
A312	1.67 ± 0.05
A412	1.46 ± 0.06
A512	0.81 ± 0.03

### 3.3 Corrosion behaviour in 3.5 % NaCl solution

Figure 3 shows the variation of mass loss (Fig. 3a) and corrosion rate (Fig. 3b) with exposure time in 3.5 wt% NaCl solution for the control composite samples which were not subjected to thermal cycling. It is observed from Fig. 3(a) that virtually all the samples have negative mass loss values for the entire period of immersion in the NaCl solution. This is an indication of weight gain by the composites samples during the immersion period which suggests that the passive protective films formed on the surface of the samples are stable. It is also observed that the Al<sub>2</sub>O<sub>3</sub> and RHA single reinforced composite samples (A10 and A50 grade) exhibited relatively higher film thickness (more weight gain) when compared with the hybrid composite grades (A20, A30 and A40). It is apparent from the figure that the hybrid mix of Al<sub>2</sub>O<sub>3</sub> and RHA in the composites did not alter the corrosion resistance capability of the Aluminium based composites when compared with the single alumina reinforced composite grade (A10). It is noted also that for the hybrid composites grades, the passive film thickness which reflects in the

composite weight gain tends to increase with increase in the RHA content in composites. The corrosion rate profiles (Fig. 3b) are noted to be in agreement with the observations from the mass loss plots (Fig. 3a). It is observed that for most of the exposure period that the corrosion rates of the composites were much lower than 0.05 mm/yr, a confirmation of the high resistance to corrosion the composites have in 3.5 % NaCl solution.

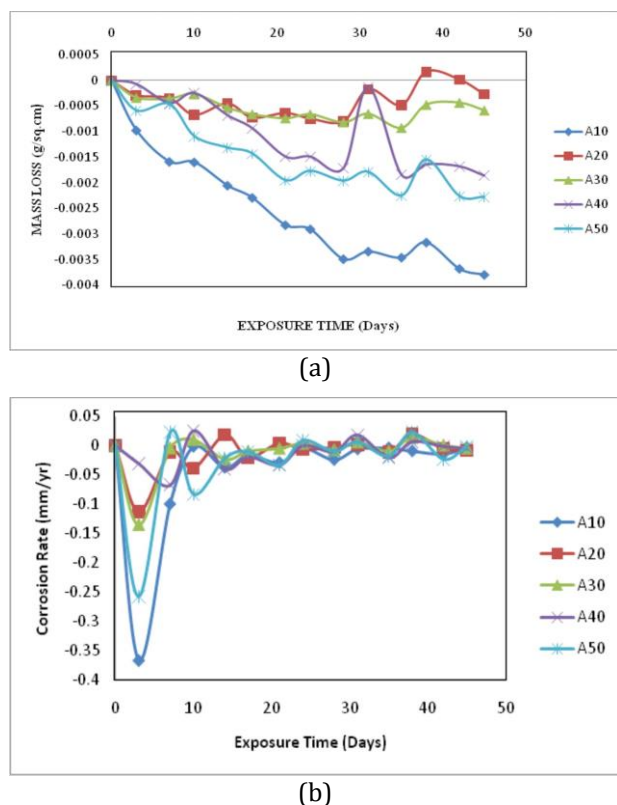


**Fig. 3.** Variation of (a) mass loss, and (b) corrosion rate with exposure time in 3.5 wt% NaCl solution for the Al-Mg-Si/Al<sub>2</sub>O<sub>3</sub>-RHA composites which were not subjected to thermal cycling.

Figure 4 show the results of the mass loss (Fig. 4a) and corrosion rate (Fig. 4b) variations with exposure time in 3.5 % NaCl solution for the single reinforced Alumina composite grades (A10) subjected to different thermal cycles. It is observed from Fig. 4(a) that the composite grades were all stable and highly resistant to corrosion in the NaCl solution judging from the negative mass loss value recorded. The single reinforced composite grade (A10) which was not subjected to repeated heating and cooling cycles is noted to have relatively thicker passive film formation (reflected by higher weight gain) compared to the thermal cycled composite grades in this series. This trend is symmetrical

with the corrosion rate profiles (Fig. 4b) where it can be confirmed that for most of the immersion periods, the composites had very low rates of corrosion in the 3.5 % NaCl solution.

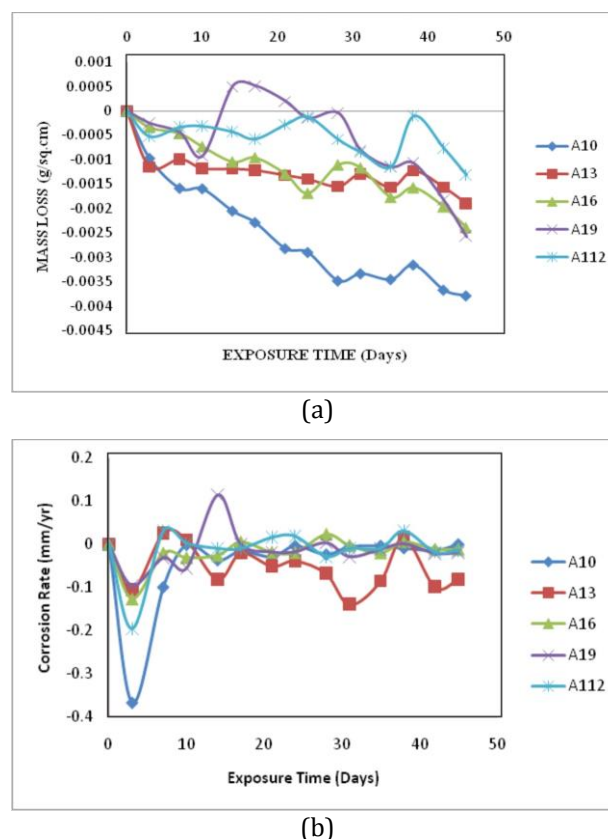


**Fig. 4.** Variation of (a) mass loss, and (b) corrosion rate with exposure time in 3.5 wt% NaCl solution for the Al/Al<sub>2</sub>O<sub>3</sub> composites subjected different thermal cycles.

In the case of the Al-Mg-Si based hybrid composites containing 75 % Al<sub>2</sub>O<sub>3</sub> and 25 % RHA (A2 grade) and subjected to different thermal cycles, the results of the mass loss and corrosion rate with exposure time in 3.5 wt% NaCl solution are presented in Fig. 5. From the mass loss plots (Fig. 5a), it is observed that the alternate heating and cooling of the composites for all cycles worked on did not have significant effect on the corrosion susceptibility of the composites as all grades maintained the same level of corrosion resistance with the composite grade not subjected to thermal cycling (A20). The exception to the general observation is the sample subjected to 9 repeated heating and cooling cycles (A29) as other composites are observed to exhibit weight gain for almost the entire period of immersion. This is an indication of stable passive film formation with little fluctuations in the film thickness. The corrosion

rate plots (Fig. 5b) confirm the generally low corrosion rates of the composites in 3.5 % NaCl solution.

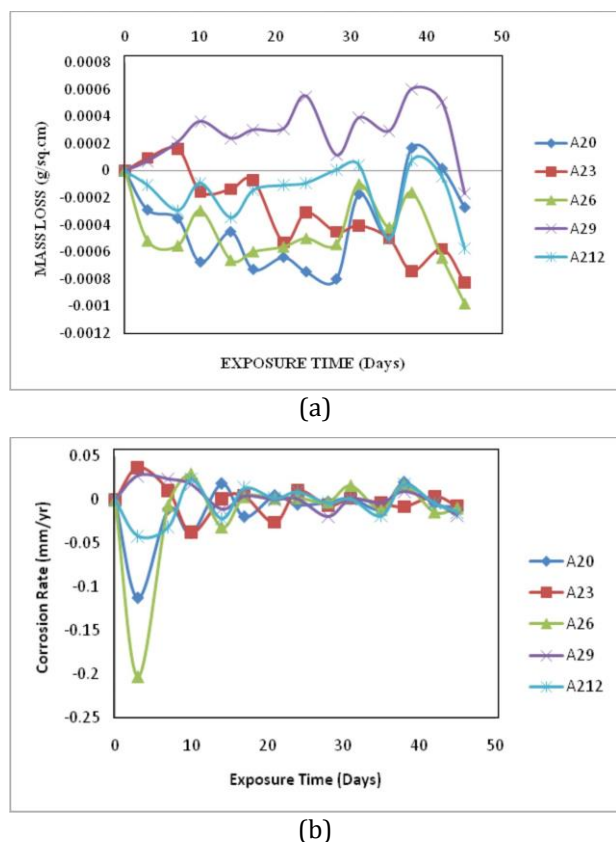


**Fig. 5.** Variation of (a) mass loss, and (b) corrosion rate with exposure time in 3.5 wt% NaCl solution for the Al-Mg-Si/75%Al<sub>2</sub>O<sub>3</sub>-25% RHA hybrid composites subjected different thermal cycles.

The results of the variation of mass loss and corrosion rates with exposure time in 3.5 wt% NaCl solution for composite series A3 (50 % Al<sub>2</sub>O<sub>3</sub>, 50 % RHA), A4 (25 % Al<sub>2</sub>O<sub>3</sub>, 75 % RHA) and A5 (100 % RHA) subjected to varied thermal cycles immersed are presented in Figs. 6-8 respectively. It is observed from the respective mass loss profiles (Figs. 6a, 7a, and 8a) that all the composite grades in each series (A3-A5) maintained a negative mass loss value throughout the period of immersion. The weight gain observed in the composite grades is indicative of high resistance to corrosion in 3.5 % NaCl solution and a reflection of stable protective film formation with continuous exposure in the NaCl solution [14]. Thus the oxide films formed are very stable and immune to the attack of the NaCl solution. The respective corrosion rate profiles (Figs. 6b, 7b, and 8b) are all observed to support the mass loss trends of their respective composite series.

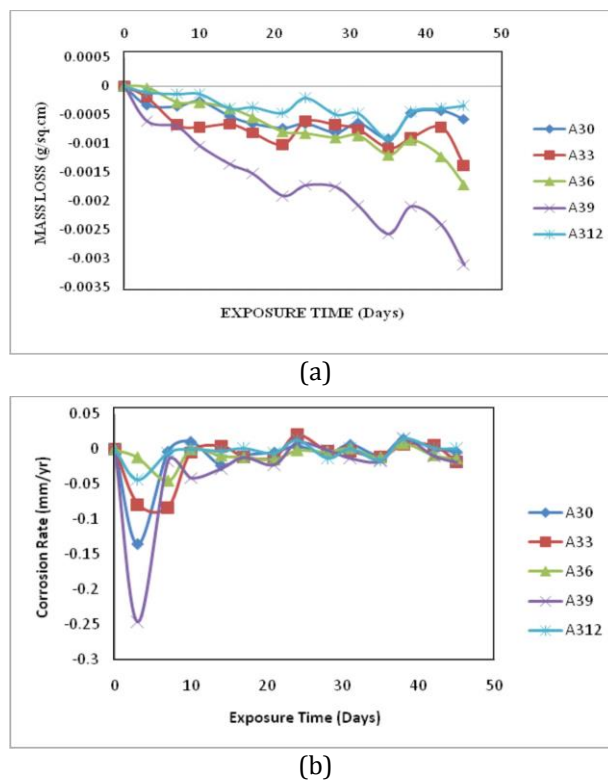


**Fig. 6.** Variation of (a) mass loss, and (b) corrosion rate with exposure time in 3.5 wt% NaCl solution for the Al-Mg-Si/50%Al<sub>2</sub>O<sub>3</sub>-50% RHA composites subjected to thermal cycling.

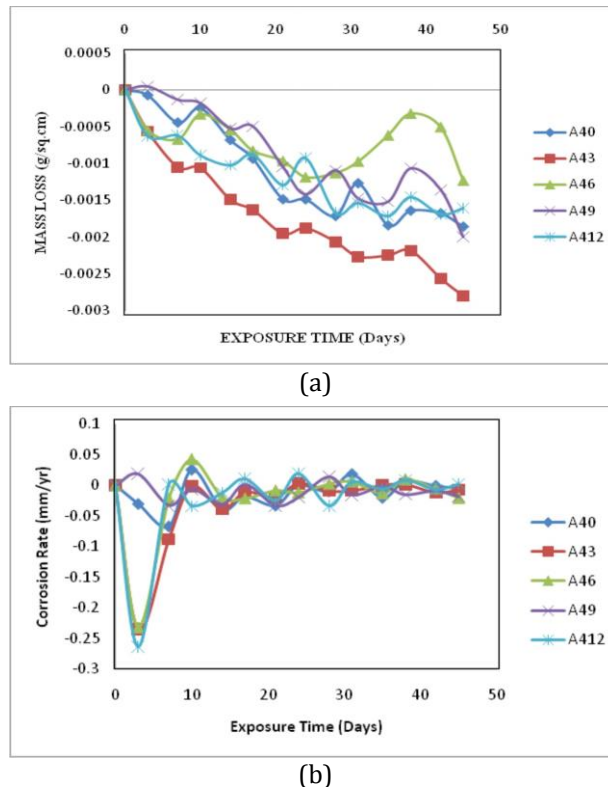


**Fig. 7.** Variation of (a) mass loss, and (b) corrosion rate with exposure time in 3.5wt% NaCl solution for the Al-Mg-Si/25 % Al<sub>2</sub>O<sub>3</sub>-75 % RHA composites subjected to thermal cycling.

Thus from the foregoing observations it is clear that the hybrid composite grades irrespective of the amount of alternate heating and cooling cycles they are subjected to in service are chemically stable in 3.5 % NaCl solution.

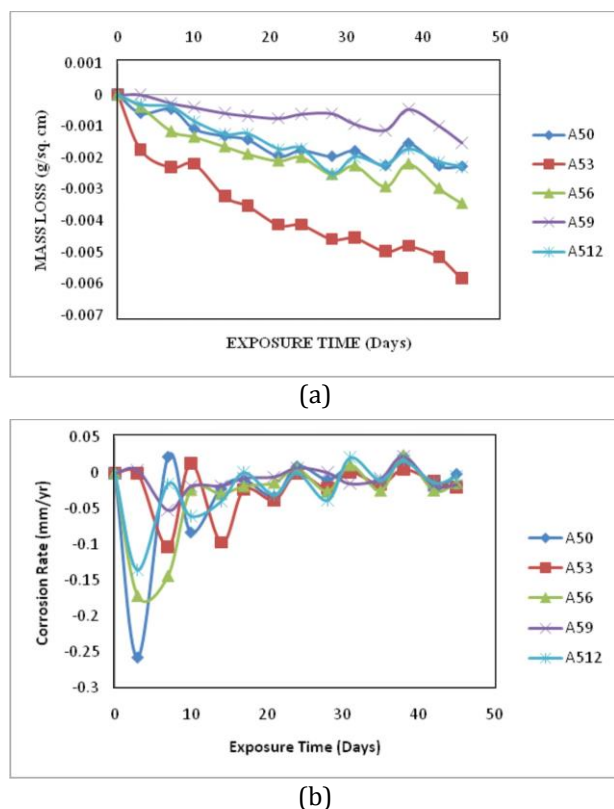


**Fig. 8.** Variation of (a) mass loss, and (b) corrosion rate with exposure time in 3.5 wt% NaCl solution for the Al-Mg-Si/RHA composites subjected to thermal cycling.

### 3.4 Corrosion behaviour in 0.3M H<sub>2</sub>SO<sub>4</sub> solution

The variation of mass loss and corrosion rate with exposure time in 0.3M H<sub>2</sub>SO<sub>4</sub> solution for the Al-Mg-Si based composites which were not subjected to thermal cycling is presented in Fig. 9. It is observed from Fig. 9(a) that the mass loss of the composites increases with immersion time in the H<sub>2</sub>SO<sub>4</sub> solution. It is also observed that the corrosion resistance of the composites improved with increase in the RHA content. This is clearly seen from the plots as the single reinforced composite grade containing 100 % RHA reinforcement (A50) exhibited the least susceptibility to corrosion in the 0.3M H<sub>2</sub>SO<sub>4</sub> solution. The corrosion rate plots (Fig. 9b) are in conformity with trends observed in the mass loss profiles (Fig. 9a). Similar corrosion behaviour has been reported in AMCs having additions of RHA [22].

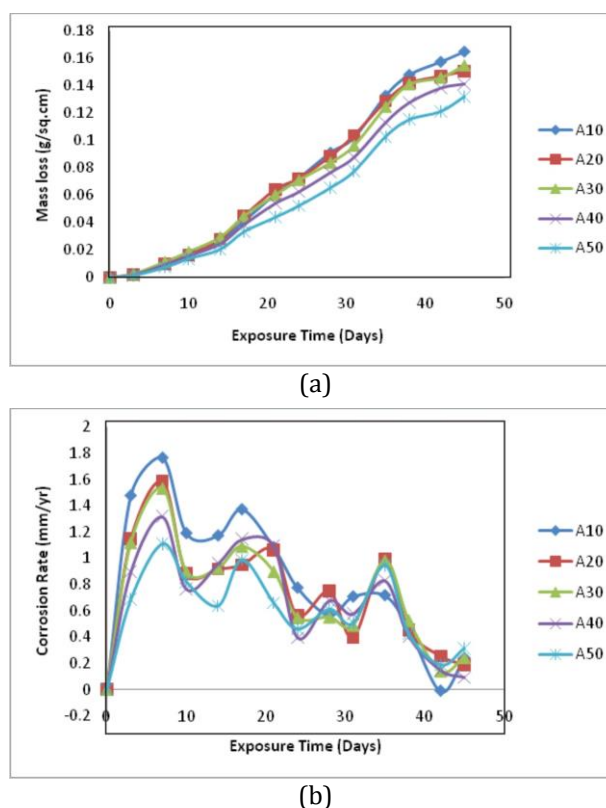
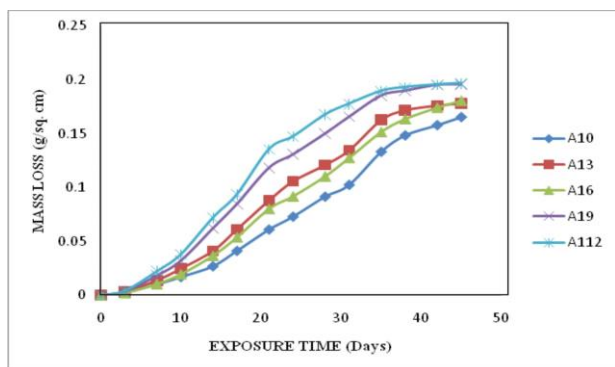
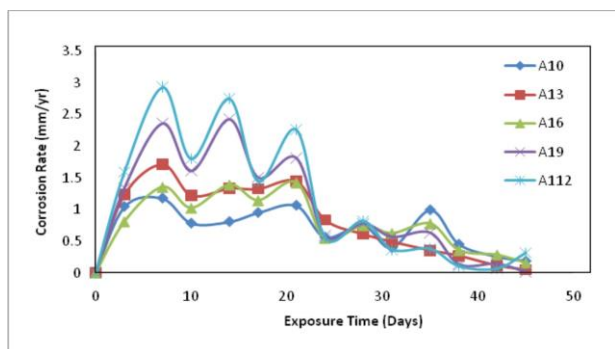


**Fig. 9.** Variation of (a) mass loss, and (b) corrosion rate with exposure time in 0.3M H<sub>2</sub>SO<sub>4</sub> solution for the Al-Mg-Si/Al<sub>2</sub>O<sub>3</sub>-RHA composites which were not subjected to thermal cycling.

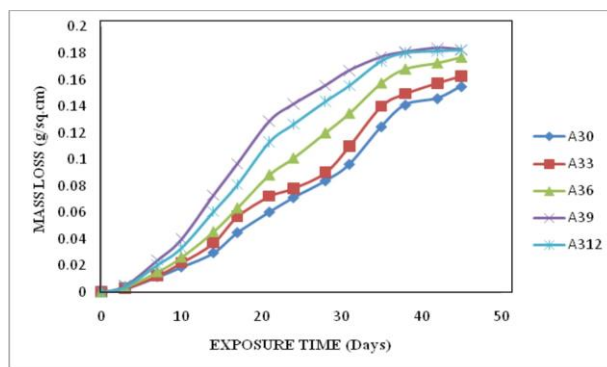
The results of the variation of mass loss and corrosion rate with exposure time in 0.3M H<sub>2</sub>SO<sub>4</sub> solution for composites A1 (containing 100 % Al<sub>2</sub>O<sub>3</sub>), A2 (75 % Al<sub>2</sub>O<sub>3</sub>, 25 % RHA), A3 (50 % Al<sub>2</sub>O<sub>3</sub>, 50 % RHA), A4 (25 % Al<sub>2</sub>O<sub>3</sub>, 75 % RHA) and A5 (100 % RHA) subjected to varied thermal cycles are presented in Figs. 10-14 respectively. In general it is observed from the respective mass loss profiles (Figs. 10a, 11a, 12a, 13a, and 14a) that all the composite series from A1-A5 follow the same trend in mass loss profile. This trend is characterized by mass loss increases with increase in exposure time irrespective of the number of thermal cycles. It is noted however that the composite grades that were not subjected to alternate heating and cooling had the highest resistance to corrosion of all the composites produced in each series (that is A10, A20, A30, A40, and A50). For all the composite series worked on, it is observed that the composite grades exposed to the highest number of thermal cycles (9 and 12 thermal cycles) appeared to be the most susceptible to corrosion in 0.3M H<sub>2</sub>SO<sub>4</sub> solution compared to the other composites in each series.



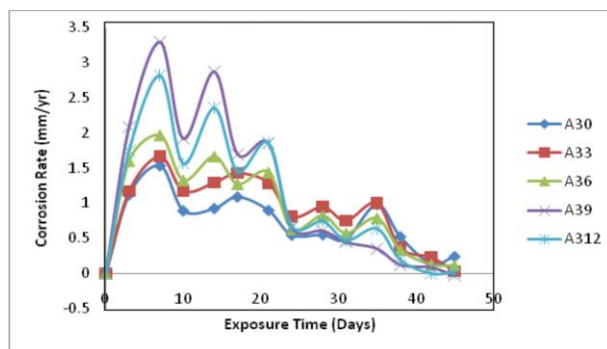
(a)



(b)



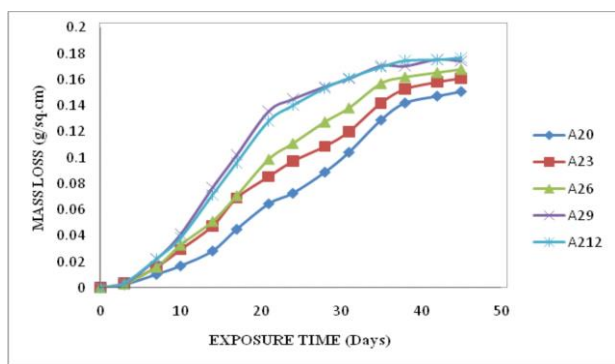
(a)



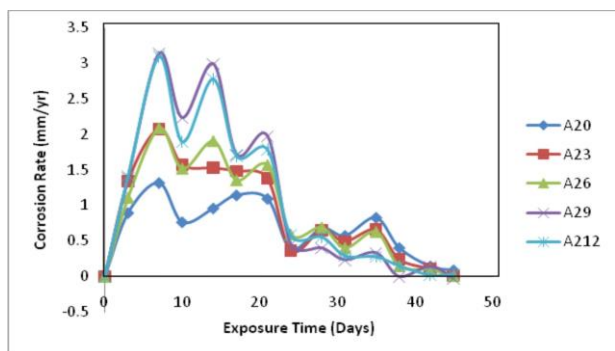
(b)

**Fig. 10.** Variation of (a) mass loss, and (b) corrosion rate with exposure time in 0.3M H<sub>2</sub>SO<sub>4</sub> solution for the Al-Mg-Si/Al<sub>2</sub>O<sub>3</sub> composites subjected different thermal cycles.

**Fig. 12.** Variation of (a) mass loss, and (b) corrosion rate with exposure time in 0.3M H<sub>2</sub>SO<sub>4</sub> solution for the Al-Mg-Si/50%Al<sub>2</sub>O<sub>3</sub>-50%RHA composites subjected different thermal cycles.

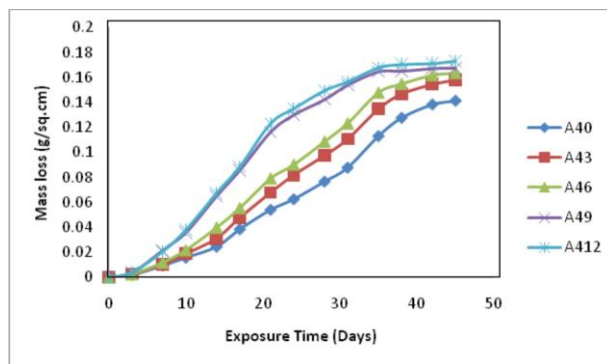


(a)

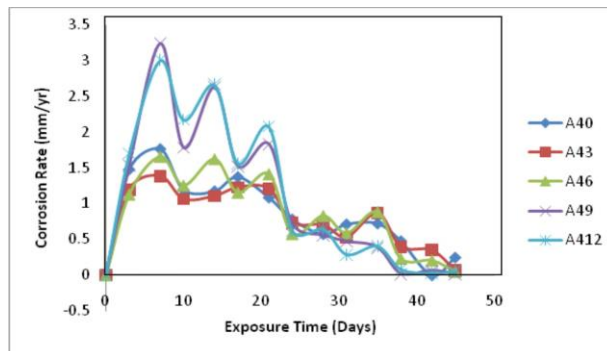


(b)

**Fig. 11.** Variation of (a) mass loss, and (b) corrosion rate with exposure time in 0.3M H<sub>2</sub>SO<sub>4</sub> solution for the Al-Mg-Si/75%Al<sub>2</sub>O<sub>3</sub>-25%RHA composites subjected different thermal cycles.

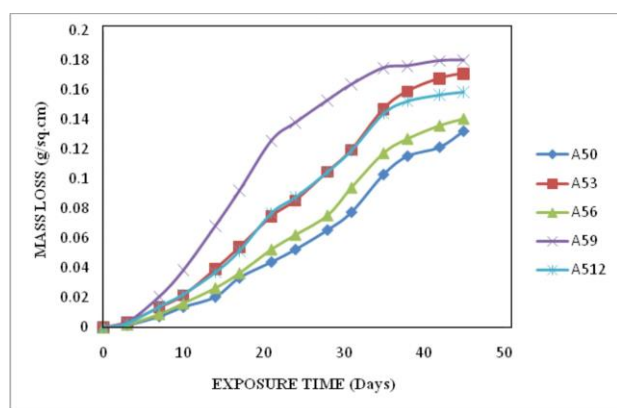


(a)

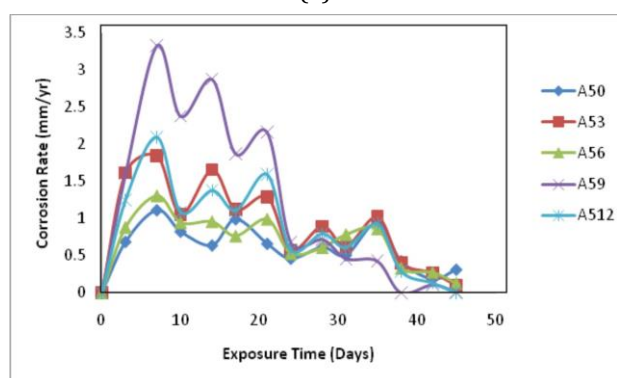


(b)

**Fig. 13.** Variation of the mass loss with exposure time in 0.3M H<sub>2</sub>SO<sub>4</sub> solution for the Al-Mg-Si/25%Al<sub>2</sub>O<sub>3</sub>-75%RHA composites subjected different thermal cycles.



(a)



(b)

**Fig. 14.** Variation of (a) mass loss, and (b) corrosion rate with exposure time in 0.3M H<sub>2</sub>SO<sub>4</sub> solution for the Al-Mg-Si/RHA composites subjected different thermal cycles.

This is an indication that the corrosion resistance of the Al based Al<sub>2</sub>O<sub>3</sub>-RHA reinforced composites degrades gradually when exposed to fluctuating thermal operating conditions in 0.3M H<sub>2</sub>SO<sub>4</sub> solution. The trends of the respective corrosion rate profiles (Figs. 10b, 11b, 12b, 13b, and 14b) are observed to be consistent with that of the mass loss profiles.

#### 4. CONCLUSION

The softening resistance, dimensional stability and corrosion behaviour of stir cast alumina and rice husk ash reinforced aluminium matrix composites subjected to thermal cycling was investigated. From the results, the following conclusions are drawn:

1. No obvious change in the microstructure could be discerned with thermal cycling of the different compositions of composites produced.

2. There were only marginal changes in hardness with increase in thermal cycling also less than 2 % change in linear dimensions was observed with thermal cycling.
3. The composites were very resistant to corrosion in 3.5 % NaCl solution with no appreciable change in corrosion resistance noted irrespective of the number of thermal cycling.
4. In 0.3M H<sub>2</sub>SO<sub>4</sub> solution, the corrosion resistance increased with increase in RHA content and samples subjected to 9 and 12 thermal cycles exhibited a relatively higher susceptibility to corrosion.

#### REFERENCE

- [1] H. Kala, K.K.S. Mer and S. Kumar, 'A Review on Mechanical and Tribological Behaviors of Stir Cast Aluminum Matrix Composites', *Procedia Materials Science*, vol. 6, pp. 1951-1960, 2014.
- [2] K.K. Alaneme and M.O. Bodunrin, 'Mechanical Behaviour of Alumina reinforced AA (6063) Metal Matrix Composites developed by two - Step Stir Casting Process', *Acta Technica Corviniensis - Bulletin of Engineering*, vol. 3, pp. 105-110, 2013.
- [3] M. Eslamian, J. Rak and N. Ashgriz, 'Preparation of aluminum/silicon carbide metal matrix composites using centrifugal atomization', *Powder Technology*, vol. 184, no. 1, pp. 11-20, 2008.
- [4] B. Vijaya Ramnath, C. Elanchezhian, M. Jaivignesh, S. Rajesh, C. Parswajinan and A.S.A. Ghias, 'Evaluation of mechanical properties of aluminium alloy-alumina-boron carbide metal matrix composites', *Materials & Design*, vol. 58, pp. 332-338, 2014.
- [5] J.M. Molina-Jordá, 'Design of composites for thermal management: Aluminum reinforced with diamond-containing bimodal particle mixtures', *Composites Part A: Applied Science and Manufacturing*, vol. 70, pp. 45-51, 2015.
- [6] M. Singla, D.D. Dwivedi, L. Singh and V. Chawla, 'Development of Aluminium Based Silicon Carbide Particulate Metal Matrix Composite', *Journal of Minerals and Materials Characterization and Engineering*, vol. 8, no.6, 455 - 467, 2009.

- [7] A. Macke, B.F. Schultz and P. Rohatgi, 'Metal matrix composites offer the automotive industry an opportunity to reduce vehicle weight, improve performance', *Advanced Materials and Processes*, vol. 170, no. 30, pp. 19-23, 2012.
- [8] S. Mallik, N. Ekere, C. Best and R. Bhatti, 'Investigation of thermal management materials for automotive electronic control units', *Applied Thermal Engineering*, vol. 31, no. 2-3, pp. 355-362, 2011.
- [9] X. Qu, L. Zhang, M. Wu and S. REN, 'Review of metal matrix composites with high thermal conductivity for thermal management applications', *Progress in Natural Science: Materials International*, vol. 21, no. 3, pp. 189-197, 2011.
- [10] G. Requena, D.C. Yubero, J. Corrochano, J. Repper and G. Garcés, 'Stress relaxation during thermal cycling of particle reinforced aluminium matrix composites', *Composites Part A: Applied Science and Manufacturing*, vol. 43, no. 11, pp. 1981-1988, 2012.
- [11] N. Chen, H. Zhang, M. Gu and Y. Jin, 'Effect of thermal cycling on the expansion behavior of Al/SiC<sub>p</sub> composite', *Journal of Materials Processing Technology*, vol. 209, no. 3, pp. 1471-1476, 2009.
- [12] L. Daguang, C. Guoqin, J. Longtao, X. Ziyang, Z. Yunhe and W. Gaohui, 'Effect of thermal cycling on the mechanical properties of Cf/Al composites', *Materials Science and Engineering: A*, vol. 586, pp. 330-337, 2013.
- [13] T. Huber, H.P. Degischer, G. Lefranc and T. Schmitt, 'Thermal expansion studies of aluminum-matrix composites with different reinforced architecture of SiC particles', *Composite Science Technology*, vol. 66, pp. 2206-2217, 2006.
- [14] K.K. Alaneme, B.O. Ademilua and M.O. Bodunrin, 'Mechanical and Corrosion Behaviour of Bamboo Leaf Ash - Silicon Carbide Hybrid Reinforced Aluminium Based Matrix Composites', *Tribology in Industry*, vol. 35, no. 1, pp. 25-35, 2013.
- [15] M.I. Pech-Canul, R. Escalera-Lozano, M. Montoya-Davila and M.A. Pech-Canul, 'The Use of Fly-ash and Rice-hull Ash in Al/SiC<sub>p</sub> Composites: A Comparative Study of the Corrosion and Mechanical Behaviour', *Revista Materia*, vol. 15, no. 1, pp. 233-239, 2010.
- [16] A. Bahrami, M.I. Pech-Canul, C.A. Gutierrez and N. Soltani, 'Effect of Rice Husk Ash on Properties of Laminated and Functionally Graded Al/SiC Composites by One-step Pressureless Infiltration', *Journal of Alloys and Compounds*, vol. 644, pp. 256-266, 2015.
- [17] K.K. Alaneme and T.M. Adewale, 'Influence of Rice husk Ash - Silicon Carbide Weight Ratios on the Mechanical Behaviour of Aluminium Matrix Hybrid Composites', *Tribology in Industry*, vol. 35, no. 2, pp. 163-172, 2013.
- [18] K.K. Alaneme and E.O. Adewuyi, 'Mechanical Behaviour of Al-Mg-Si Matrix Composites Reinforced with Alumina and Bamboo Leaf Ash', *Metallurgical and Materials Engineering*, vol. 19, no. 3, pp. 177-187, 2013.
- [19] ASTM E 92-82: *Standard Test Method for Vickers Hardness of Metallic Materials*, ASTM International, West Conshohocken, PA, 2003, [www.astm.org](http://www.astm.org)
- [20] ASTM D1204-14: *Standard Test Method for Linear Dimensional Changes of Nonrigid Thermoplastic Sheet or Film at Elevated Temperature*, ASTM International, West Conshohocken, PA, 2014, [www.astm.org](http://www.astm.org), DOI: 10.1520/D1204.
- [21] ASTM NACE / ASTM G31-12a: *Standard Guide for Laboratory Immersion Corrosion Testing of Metals*, ASTM International, West Conshohocken, PA, 2012, [www.astm.org](http://www.astm.org), DOI: 10.1520/G0031-12A.
- [22] K.K. Alaneme, I.B. Akintunde, P.A. Olubambi and T.M. Adewale, 'Mechanical behaviour of rice husk ash—alumina hybrid reinforced aluminium based matrix composites', *Journal of Materials Research and Technology*, vol. 2, no.1, pp. 60-67, 2013.